ACS Macro Letters

Letter

pubs.acs.org/macroletters

Mechanically Linked Poly[2]rotaxanes Constructed via the Hierarchical Self-Assembly Strategy

Yonggang Shi, Zhishuai Yang, Huaqing Liu, Zijian Li, Yukui Tian, and Feng Wang*

Key Laboratory of Soft Matter Chemistry, Collaborative Innovation Center of Chemistry for Energy Materials, Department of Polymer Science and Engineering, University of Science and Technology of China, Hefei, Anhui 230026, People's Republic of China

Supporting Information

ABSTRACT: Mechanically linked poly[2]rotaxanes have been successfully constructed via the hierarchical self-assembly strategy. The integration of two noninterfering noncovalent recognition motifs facilitates chain extension of the B21C7-based [2]rotaxane monomer, demonstrating the capabilities to form self-standing films with preferable transparency and softness.

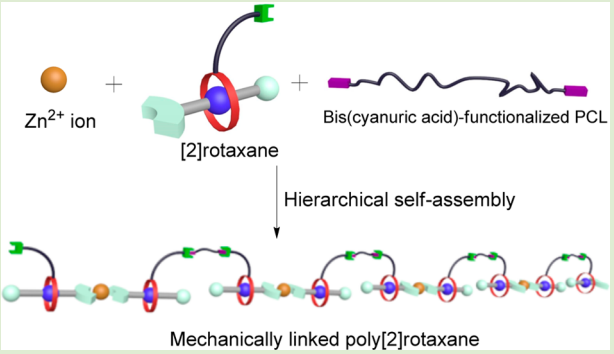

Polyrotaxanes have attracted increasing attention due to their unique topological architectures and fascinating properties.[1] Traditionally, polyrotaxanes are fabricated via encircling an already existing polymer with a variety of macrocycles (Scheme 1a).[2] As compared with such main-chain poly[*n*]rotaxanes, mechanically linked polyrotaxanes, representing the embedment of mechanical bonds as integral parts of the polymer backbone, impart unusual rotational and elongational mobility to the polymeric chain and thereby display unique rheological behaviors.[3] In this respect, poly[*c*2]-daisy chains (Scheme 1b), which have been elegantly developed by Stoddart and Giuseppone et al., realize the conversion from nanoscale mechanical movement to macroscopic muscle-like function.[4] However, the [*c*2]daisy chain involved in the structures commonly suffers from tedious preparation and low reaction yield. Additionally, high structural symmetry of the [*c*2]daisy chain restricts the formation of advanced supramolecular architectures. To solve this issue, an alternative choice is to utilize [2]rotaxane as the basic building block, which is more easily available than the [*c*2]daisy chain counterpart. Remarkably, different functional groups could be introduced asymmetrically on the axle and wheel sites of the [2]rotaxane scaffold, facilitating the subsequent polymerization steps.[5] For example, Takata et al. have demonstrated the efficient fabrication of linear poly[2]rotaxanes with the utilization of Sonogashira polycondensation reaction.[5a]

Besides the traditional covalent polymerization methodology, mechanically linked polyrotaxanes could also be achieved via the noncovalent self-assembly strategy. It is worthy of note that such a hierarchical self-assembling protocol could not only inherit the intrinsic viscoelastic properties of the conventional polyrotaxanes, but also possess some novel behaviors. For example, the dynamic features of the implemented noncovalent recognition motifs significantly influence the physical properties of the mechanically linked polyrotaxanes, benefiting for exploring their adaptivity toward external stimuli.[6] Furthermore, various functional elements could be incorporated in a modular way, thus considerably enriching the complexity for the resulting supramolecular assemblies with integrated functionality.[7]

In this manuscript, we sought to decorate the [2]rotaxane scaffold with two different supramolecular recognition groups, and furthermore realize the formation of mechanically linked poly[2]rotaxanes via the hierarchical self-assembly strategy. Specifically, the [2]rotaxane **2** (Scheme 1c) is first prepared based on the benzo-21-crown-7 (B21C7)/secondary ammonium salt recognition motif, which possesses relatively strong binding affinity (association constant $K_a \sim 10^3$ M^{-1} in acetone at room temperature).[8] On this basis, terpyridine unit is anchored on the axle of the [2]rotxane scaffold, which is prone to form the dimeric supramolecular [3]rotaxane **4** (Scheme 1c) upon addition of transition metal ions, such as Zn^{2+}.[9] Meanwhile, Hamilton receptor, locating on the wheel of the [2]rotaxane **2**, is expected to form stable hydrogen-bonding complex **3** (Scheme 1c) with the complementary homoditopic cyanuric acid-functionalized polycaprolactone (PCL) **1**.[10] If the involved hydrogen bonding and metal−ligand interactions are verified to be totally noninterfering, mixing all of the three compounds together should lead to the desired mechanically linked poly[2]rotaxanes **5** (Scheme 1c).

Received: October 16, 2014
Accepted: December 5, 2014
Published: December 10, 2014

   dx.doi.org/10.1021/mz500659f | *ACS Macro Lett.* 2015, 4, 6−10

Scheme 1. Schematic Representation for (a) Main-Chain Poly[*n*]rotaxanes, (b) Poly[*c*2]daisy Chains, and (c) Hierarchical Construction of Mechanically Linked Poly[2]rotaxanes 5

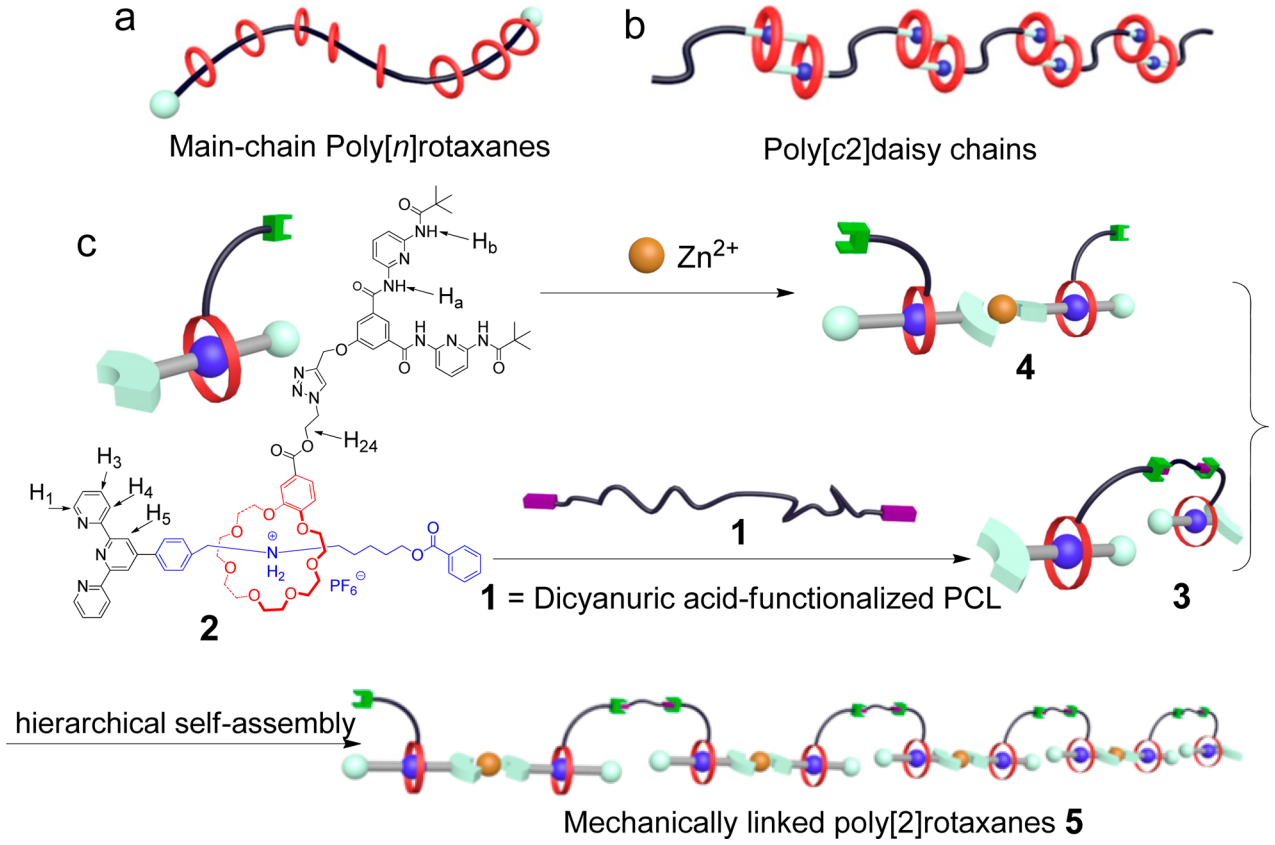

Scheme 2. Synthetic Routes to the Monomers 1 and 2

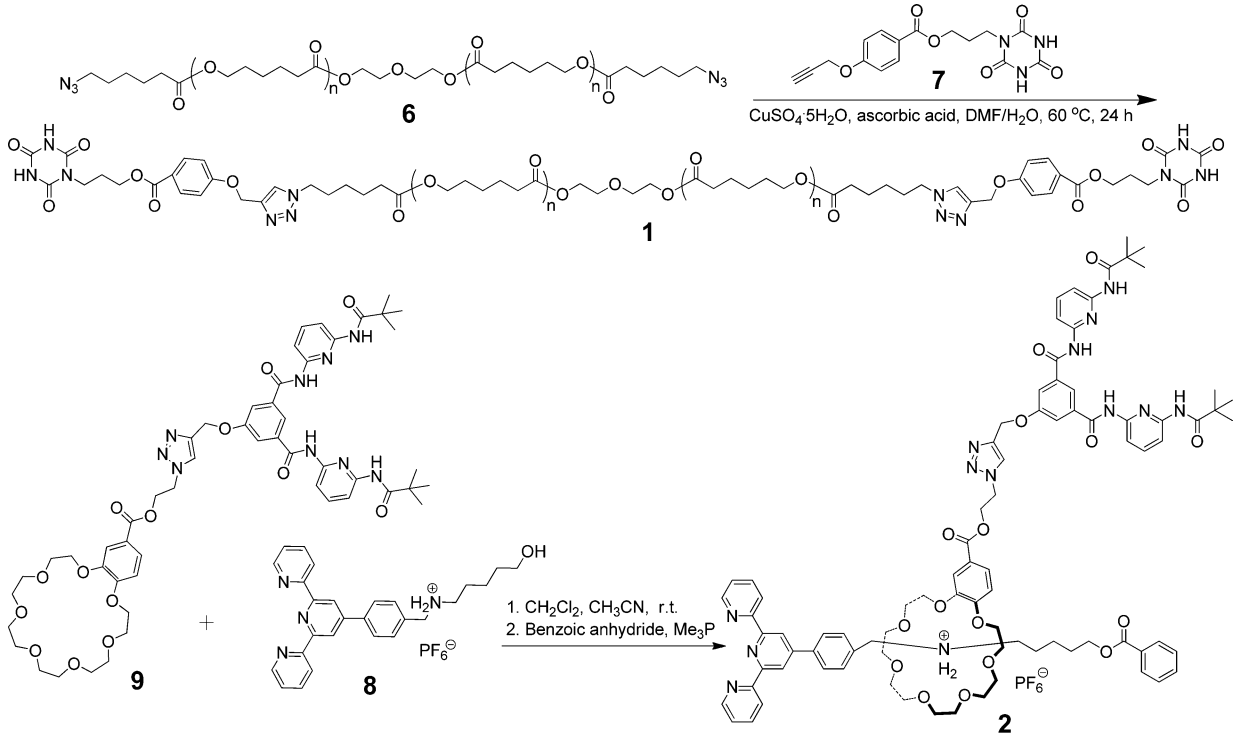

For the synthesis of the monomer **1** bearing two cyanuric acid units on both sides, copper(I)-catalyzed click reaction was performed between PCL–N_3 **6** and excess amount of cyanuric acid **7** (Scheme 2). Complete conversion of **6** to **1** is verified by the disappearance of the methylene protons on **6** (δ = 3.27 ppm), as well as the emergence of the triazole signal (δ = 7.63

dx.doi.org/10.1021/mz500659f | ACS Macro Lett. 2015, 4, 6−10

ppm) in the ^{1}H NMR spectra (SI, Figure S7c,d). On the other hand, the [2]rotaxane **2**, functionalized on both the wheel and stopper positions, is efficiently synthesized via the "threading-followed-by-stoppering" strategy (Scheme 2).[8a] Briefly, the terpyridine-decorated axle **8**, which is slightly soluble in CH_2Cl_2, becomes soluble upon mixing with equimolar amount of the wheel **9**, suggesting the formation of [2]pseudorotaxane threaded structure. Further addition of benzoic anhydride to the host−guest binary mixture and stirring at room temperature for 1 day furnish the desired monomer **2** in 72% yield.

The electrospray ionization mass spectrometry for **2** displays an intense peak at m/z 1569.0 (SI, Figure S19), corresponding to the species $[\mathbf{2} - PF_6]^+$, thus, validating the formation of threaded [2]rotaxane structure in the gaseous phase. ^{1}H NMR measurement is also performed to illustrate the mechanically interlocked property of **2**. As compared with the respective axle **8** and wheel **9** (Figure 1a,b), it is evident that, after the formation of [2]rotaxane, proton H_{24} neighboring to the B21C7 unit show noticeable upfield shift, while the original four sets of ethyleneoxy protons on the B21C7 moiety exhibit remarkable peak-splitting behaviors, ascribing to the symmetry breaking effect. Although the 1:1 mixture of **8** and **9** exhibits both complexed and uncomplexed signals for the B21C7/secondary ammonium salt recognition motif (SI, Figure S20b), only complexed ^{1}H NMR peaks are observed for the [2]rotaxane **2** on the ^{1}H NMR time scale (Figure 1c). Such phenomena demonstrate that dethreading of the B21C7 ring from the axle could be totally suppressed due to the existence of the phenyl stoppers. Furthermore, DMSO-d_6 is utilized instead of CD_3CN to prove the stability of the mechanically interlocked structure (Figure 1d). The resulting ^{1}H NMR spectrum of **2** shows severe peak-splitting behavior, similar to that observed in CD_3CN, supporting the maintenance of the [2]rotaxane structure in such a highly polar solvent.

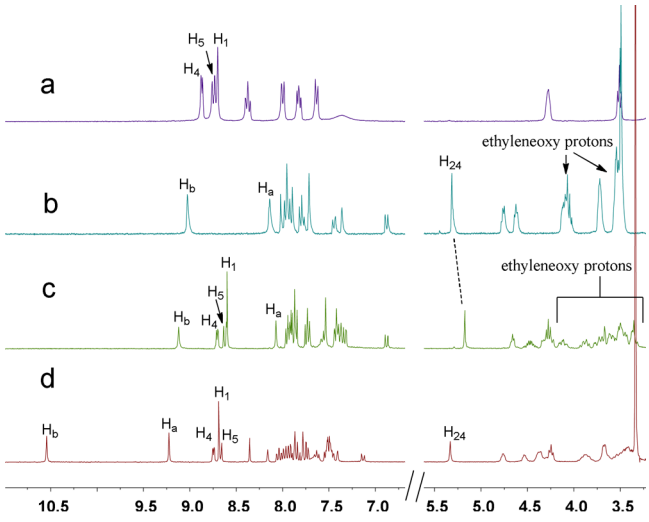

Figure 1. Partial ^{1}H NMR spectra (400 MHz, 293 K) of (a) 2.00 mM **8**, (b) 2.00 mM **9**, (c) 2.00 mM [2]rotaxane **1** in CD_3CN, and (d) 2.00 mM **1** in DMSO-d_6.

Hydrogen-bonding complexation between the Hamilton receptor of **2** and the complementary cyanuric acid derivatives is elucidated via ^{1}H NMR measurements. The monotopic cyanuric acid compound **10** (SI, Figure S21) is demonstrated to form stable 1:1 complex with **2** in $CHCl_3/CH_3CN$ (v/v = 2:1). Considering that monomer **1** consists of two cyanuric acid moieties, stepwise addition of **2** (from 0 to 0.84 equiv) to **1** leads to the substantial downfield shifts for both of the NH signals on **2** (H_a and H_b: from 8.07 and 8.76 ppm to 8.38 and 9.09 ppm, respectively) (SI, Figure S22). The molar ratio plot, derived from ^{1}H NMR titration experiments, provides the clear evidence for 1:2 binding stoichiometry between **1** and **2** (Figure 2a). Noteworthy, no obvious chemical shift change occurs for the terpyridine protons $H_{1,4-5}$ during the titration experiments, suggesting the preferential hydrogen bonding complexation without the participation of the terpyridine moiety.

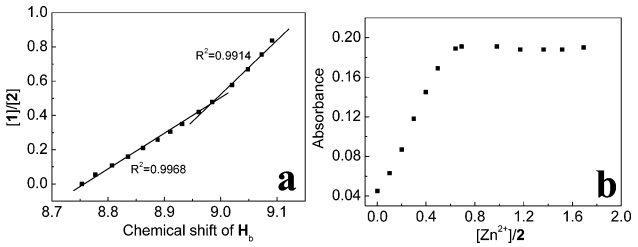

Figure 2. (a) Mole ratio plot between **1** and **2** derived from ^{1}H NMR titration experiments (300 MHz, $CDCl_3/CD_3CN$ (v/v, 2:1), 293 K). (b) UV/vis titration data (345 nm) upon gradual addition of $Zn(OTf)_2$ to **2**.

Meanwhile, metal−ligand coordination behavior between [2]rotaxane **2** and Zn^{2+} was monitored by means of UV/vis spectroscopy. Briefly, stepwise titration of $Zn(OTf)_2$ (1×10^{-3} M) to **2** (2×10^{-5} M) in $CHCl_3/CH_3CN$ (v/v = 2:1) exhibits a clear isosbestic point at 320 nm (SI, Figure S23a), indicating the transition from free to metal-complexed terpyridine species. The achievement of the maximum absorbance band (λ = 345 nm) at the $Zn(OTf)_2$/**2** molar ratio of 0.5 indicates the formation of stable 1:2 dimeric complex **4** (Figure 2b). Stimuli-responsive properties of the resulting supramolecular [3]-rotaxane **4** are further investigated via gradual addition of cyclen (1,4,7,10-tetraazacyclododecane).[11] It is evident that adding 1.6 equiv of cyclen leads to the total disappearance of the Zn^{2+}/terpyridine absorption bands (λ_{max} = 345 nm), reflecting the breakup of the Zn^{2+}/terpyridine complexation due to the involvement of a competitive Zn^{2+}-chelating ligand (SI, Figure S24a,c). Successive addition of $Zn(OTf)_2$ results in the reappearance of the Zn^{2+}/terpyridine absorption band in UV−vis spectrum. Such phenomena suggest the total restore of metal−ligand coordination interactions, which is not interfered by the presence of telechelic PCL **1** (SI, Figure S24b,c).

It should be noted that, for the achievement of mechanically linked polyrotaxanes **5** via hierarchical self-assembly process, high-fidelity complexation between terpyridine−Zn^{2+} and Hamilton receptor/cyanuric acid recognition motifs is required. Hence, terpyridine, $Zn(OTf)_2$, Hamilton receptor **11**, and cyanuric acid **1** are served as the model compounds, which were mixed together with 2:1:2:1 ratio and submitted for ^{1}H NMR measurements (SI, Figure S25). The resulting spectrum for the four-component mixture almost overlaps the spectra of the respective metal−ligand and hydrogen−bonding complexes, definitely supporting their orthogonal complexation characters.

Subsequently, we turned to construct the desired mechanically linked polyrotaxanes **5**, by simultaneous embedment of the metal−ligand and hydrogen−bonding interactions via "one-pot" mixing of 1:2:1 mixture of monomers **1**, **2**, and $Zn(OTf)_2$

dx.doi.org/10.1021/mz500659f | ACS Macro Lett. 2015, 4, 6−10

in chloroform/acetonitrile (v/v = 2:1) solution. Concentration-dependent ^{1}H NMR measurements (Figure 3) reveal the

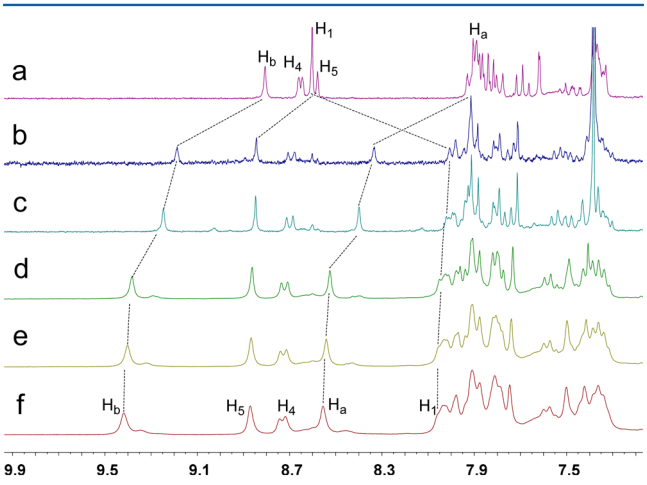

Figure 3. Partial ^{1}H NMR spectra (300 MHz, $CDCl_3/CD_3CN$ (v/v, 2:1), 293 K) of (a) monomer **2**; and the poly[2]rotaxanes **5** constructed by 1:2:1 mixture of monomers **1**, **2**, and $Zn(OTf)_2$ at different monomer **2** concentrations: (b) 1.0; (c) 5.0; (d) 10.0; (e) 20.0; (f) 40.0 mM.

formation of Zn^{2+}−terpyridine coordination complexes for all the measured concentrations, as evidenced by the obvious downfield shifts for H_5 and upfield shifts for H_1. Such phenomena could be attributed to the high thermodynamic stability of Zn^{2+}−terpyridine complex (association constant > 10^8 M^{-1}).[9a] Nevertheless, hydrogen bonding interactions between Hamilton receptor and cyanuric acid moieties considerably strengthen upon increasing the monomer concentration from 1 to 10 mM (Figure 3b−d), which is reflected by the significant downfield shifts for protons $H_{a,b}$ on the Hamilton receptor. Slighter changes occur for further increasing the monomer concentration (Figure 3d−f), indicating that the high-molecular-weight polymeric assemblies prevail above such a critical point. The concentration-dependent size variation is directly probed via DOSY (two-dimensional diffusion-ordered NMR) measurements (SI, Figure S26). As the monomer concentration of **2** increases from 5.00 to 60.0 mM, the measured diffusion coefficients decrease dramatically from 3.18×10^{-10} to 3.38×10^{-11} m^2 s^{-1}. Hence, it is obvious that increasing the monomer concentration is advantageous for the formation of linear poly[2]rotaxanes aggregates.

Capillary viscosity measurements were further employed to investigate the concentration-dependent rheological properties of **5**. For 1:2:1 mixture of monomers **1**, **2**, and $Zn(OTf)_2$ in the concentration range of 1−20 mM, the variation of specific viscosity as a function of monomer concentration changes exponentially (Figure 4a), supporting the formation of polyrotaxane species at high concentration. With the monomer concentration exceeding 30 mM, the solution is too viscous to record any valid data by the Ubbelohde viscometer (0.47 mm inner diameter), implying the significant physical entanglements for the resulting assemblies. In sharp contrast, plotting the specific viscosities of the binary mixtures **3** and **4** provides shallow curves (Figure 4a), thus, indicating that either metal−ligand or hydrogen-bonding motif plays the crucial role in the supramolecular polymerization process. Notably, based on the double logarithmic plot of specific viscosity versus concentration, the CPC (critical polymerization concentration) value is determined as 7 mM (SI, Figure S27), which is highly consistent with the above ^{1}H NMR results. Such a relative low CPC value denotes that, due to the presence of flexible PCL unit, the conformation of the neighboring noncovalent complexation would not be restricted, which benefits for the transition from the cyclic oligomers to the linear species.[12]

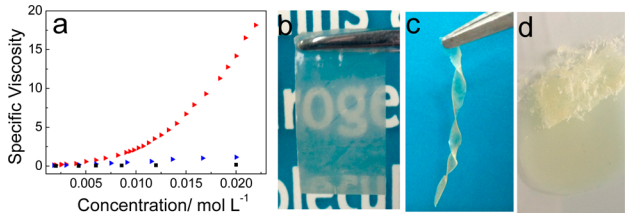

Figure 4. (a) Specific viscosities of mechanically linked polyrotaxanes **5** (red triangle), hydrogen−bonding dimeric complex **3** (blue triangle), and supramolecular [3]rotaxane complexes **4** (■) as a function of monomer **2** concentration ($CHCl_3/CH_3CN$ (2:1, v/v), 293 K). (b, c) Transparent and soft films derived from mechanically linked polyrotaxanes **5**. (d) Fragile film derived from the telechelic PCL **1**.

Self-standing films were further fabricated by solution casting of the 1:2:1 mixture of monomers **1**, **2**, and $Zn(OTf)_2$ ($CHCl_3/CH_3CN$ (2:1, v/v)) at high monomer concentration. Based on the differential scanning calorimetry (DSC) measurements, the resulting films display a melting transition at 46.2 °C (SI, Figure S28c), which is a little lower than the corresponding PCL-diol and **1** (48.6 and 49.0 °C, respectively; SI, Figure S28a,b). Additionally, no obvious crystallization peak could be visualized for the supramolecular films derived from **5**, while the crystallization peaks for both PCL-diol and **1** are located at 26.6 and 11.9 °C, respectively. Such phenomena are primarily ascribed to the existence of Hamilton receptor/cyanuric acid hydrogen bonding interactions, which influence the thermal properties of the parent PCL polymers. Furthermore, it is worth mentioning that the resulting self-standing film derived from **5** possesses a preferable transparency and softness properties, facilitating to mold its shape with the utilization of the blade (Figure 4b,c). In contrast, the film derived from the telechelic PCL **1** is more fragile (Figure 4d), indicating that chain extension via noncovalent linkage could effectively modulate the film brittleness.

In summary, we have successfully constructed supramolecular poly[2]rotaxanes **5** via the hierarchical self-assemble strategy. The integration of two orthogonal noncovalent interactions into the B21C7-based [2]rotaxane monomer facilitates the chain extension, which demonstrates the capabilities to form self-standing films. The novel types of mechanically linked polyrotaxanes, which are regulated in a facile and controlled manner, motivate us to explore their potential applications as processable materials in the near future.

■ ASSOCIATED CONTENT

Supporting Information

Full experimental details and characterization data. This material is available free of charge via the Internet at http://pubs.acs.org.

dx.doi.org/10.1021/mz500659f | ACS Macro Lett. 2015, 4, 6−10

AUTHOR INFORMATION

Corresponding Author

*E-mail: drfwang@ustc.edu.cn.

Notes

The authors declare no competing financial interest.

ACKNOWLEDGMENTS

This work was supported by the National Natural Science Foundation of China (21274139, 91227119) and the Fundamental Research Funds for the Central Universities (WK2060200012, WK2060200010).

REFERENCES

(1) (a) Takata, T.; Kihara, N.; Furusho, Y. *Adv. Polym. Sci.* **2004**, *171*, 1−75. (b) Huang, F.; Gibson, H. W. *Prog. Polym. Sci.* **2005**, *30*, 982−1018. (c) Fang, L.; Olson, M. A.; Benitez, D.; Tkatchouk, E.; Goddard, W. A., III; Stoddart, J. F. *Chem. Soc. Rev.* **2010**, *39*, 17−29. (d) Arunachalam, M.; Gibson, H. W. *Prog. Polym. Sci.* **2014**, *39*, 1043−1073.

(2) (a) Frampton, M. J.; Anderson, H. L. *Angew. Chem., Int. Ed.* **2007**, *46*, 1028−1064. (b) Liao, X.; Chen, G.; Liu, X.; Chen, W.; Chen, F.; Jiang, M. *Angew. Chem., Int. Ed.* **2010**, *49*, 4409−4413. (c) Tamura, A.; Yui, N. *Chem. Commun.* **2014**, *50*, 13433−13446. (d) Song, Q.; Luo, Z.; Tong, X.; Du, Y.; Huang, Y. *Chin. J. Polym. Sci.* **2014**, *32*, 1003−1009.

(3) Rowan, S. J.; Stoddart, J. F. *Polym. Adv. Technol.* **2002**, *13*, 777−787.

(4) (a) Fang, L.; Hmadeh, M.; Wu, J.; Olson, M. A.; Spruell, J. M.; Trabolsi, A.; Yang, Y.-W.; Elhabiri, M.; Albrecht-Gary, A.-M.; Stoddart, J. F. *J. Am. Chem. Soc.* **2009**, *131*, 7126−7134. (b) Du, G.; Moulin, E.; Jouault, N.; Buhler, E.; Giuseppone, N. *Angew. Chem., Int. Ed.* **2012**, *51*, 12504−12508. (c) Gao, L.; Zhang, Z.; Zheng, B.; Huang, F. *Polym. Chem.* **2014**, *5*, 5734−5739.

(5) (a) Sasabe, H.; Inomoto, N.; Kihara, N.; Suzuki, Y.; Ogawa, A.; Takata, T. *J. Polym. Sci., Part. A: Polym. Chem.* **2007**, *45*, 4154−4160. (b) Lee, Y.-G.; Koyama, Y.; Yonekawa, M.; Takata, T. *Macromolecules* **2010**, *43*, 4070−4080. (c) De Bo, G.; De Winter, J.; Gerbaux, P.; Fustin, C.-A. *Angew. Chem., Int. Ed.* **2011**, *50*, 9093−9096. (d) Aoki, D.; Uchida, S.; Takata, T. *ACS Macro Lett.* **2014**, *3*, 324−328.

(6) (a) Yan, X.; Wang, F.; Zheng, B.; Huang, F. *Chem. Soc. Rev.* **2012**, *41*, 6042−6065. (b) Liu, K.; Kang, Y.; Wang, Z.; Zhang, X. *Adv. Mater.* **2013**, *25*, 5530−5548.

(7) (a) Zhang, Z.; Luo, Y.; Chen, J.; Dong, S.; Yu, Y.; Ma, Z.; Huang, F. *Angew. Chem., Int. Ed.* **2011**, *50*, 1397−1401. (b) Dong, S.; Zheng, B.; Xu, D.; Yan, X.; Zhang, M.; Huang, F. *Adv. Mater.* **2012**, *24*, 3191−3195. (c) Ji, X.; Yao, Y.; Li, J.; Yan, X.; Huang, F. *J. Am. Chem. Soc.* **2013**, *135*, 74−77. (d) Li, J.; Wei, P.; Wu, X.; Xue, M.; Yan, X. *Org. Lett.* **2013**, *15*, 4984−4987. (e) Xing, H.; Wei, P.; Yan, X. *Org. Lett.* **2014**, *16*, 2850−2853. (f) Elacqua, E.; Lye, D. S.; Weck, M. *Acc. Chem. Res.* **2014**, *47*, 2405−2416.

(8) (a) Zhang, C.; Li, S.; Zhang, J.; Zhu, K.; Li, N.; Huang, F. *Org. Lett.* **2007**, *9*, 5553−5556. (b) Yan, X.; Xu, D.; Chi, X.; Chen, J.; Dong, S.; Ding, X.; Yu, Y.; Huang, F. *Adv. Mater.* **2012**, *24*, 362−369. (c) Zhang, M.; Xu, D.; Yan, X.; Chen, J.; Dong, S.; Zheng, B.; Huang, F. *Angew. Chem., Int. Ed.* **2012**, *51*, 7011−7015. (d) Jiang, W.; Nowosinski, K.; Loew, N. L.; Dzyuba, E. V.; Klautzsch, F.; Schaefer, A.; Huuskonen, J.; Rissanen, K.; Schalley, C. A. *J. Am. Chem. Soc.* **2012**, *134*, 1860−1868. (e) Tian, Y.-K.; Yang, Z.-S.; Lv, X.-Q.; Yao, R.-S.; Wang, F. *Chem. Commun.* **2014**, *50*, 9477−9480.

(9) (a) Shunmugam, R.; Gabriel, G. J.; Aamer, K. A.; Tew, G. N. *Macromol. Rapid Commun.* **2010**, *31*, 784−793. (b) Burnworth, M.; Tang, L.; Kumpfer, J. R.; Duncan, A. J.; Beyer, F. L.; Fiore, G. L.; Rowan, S. J.; Weder, C. *Nature* **2011**, *472*, 334−337. (c) Happ, B.; Winter, A.; Hagerabc, M. D.; Schubert, U. S. *Chem. Soc. Rev.* **2012**, *41*, 2222−2255. (d) Tian, Y.-K.; Shi, Y.-G.; Yang, Z.-S.; Wang, F. *Angew. Chem., Int. Ed.* **2014**, *53*, 6090−6094.

(10) Yang, S. K.; Ambade, A. V.; Weck, M. *J. Am. Chem. Soc.* **2010**, *132*, 1637−1645.

(11) Tian, Y.-K.; Wang, F. *Macromol. Rapid Commun.* **2014**, *35*, 337−343.

(12) De Greef, T. F. A.; Smulders, M. M. J.; Wolffs, M.; Schenning, A. P. H. J.; Sijbesma, R. P.; Meijer, E. W. *Chem. Rev.* **2009**, *109*, 5687−5754.